Title
Long-term O3–precursor relationships in Hong Kong: field observation and model simulation

Journal
Atmospheric Chemistry and Physics, 17(18)

ISSN
1680-7316

Authors
Wang, Yu
Wang, Hao
Guo, Hai
et al.

Publication Date
2017

DOI
10.5194/acp-17-10919-2017

Atmos. Chem. Phys., 17, 10919–10935, 2017
https://doi.org/10.5194/acp-17-10919-2017

Atmospheric Chemistry and Physics
Open Access
EGU

Long-term O_3–precursor relationships in Hong Kong: field observation and model simulation

Yu Wang[1,*], Hao Wang[1,*], Hai Guo[1], Xiaopu Lyu[1], Hairong Cheng[2], Zhenhao Ling[3], Peter K. K. Louie[4], Isobel J. Simpson[5], Simone Meinardi[5], and Donald R. Blake[5]

[1]Air Quality Studies, Department of Civil and Environmental Engineering, the Hong Kong Polytechnic University, Hong Kong SAR, China
[2]Department of Environmental Engineering, School of Resource and Environmental Sciences, Wuhan University, Wuhan 430079, China
[3]School of Atmospheric Sciences, Sun Yat-sen University, Guangzhou, China
[4]Air Group, Hong Kong Environmental Protection Department, Hong Kong SAR, China
[5]Department of Chemistry, University of California, Irvine, CA, USA
[*]These authors contributed equally to this work.

Correspondence to: Hai Guo (ceguohai@polyu.edu.hk) and Hairong Cheng (chenghr@whu.edu.cn)

Received: 13 March 2017 – Discussion started: 14 March 2017
Revised: 24 July 2017 – Accepted: 16 August 2017 – Published: 15 September 2017

Abstract. Over the past 10 years (2005–2014), ground-level O_3 in Hong Kong has consistently increased in all seasons except winter, despite the yearly reduction of its precursors, i.e. nitrogen oxides ($NO_x = NO + NO_2$), total volatile organic compounds (TVOCs), and carbon monoxide (CO). To explain the contradictory phenomena, an observation-based box model (OBM) coupled with CB05 mechanism was applied in order to understand the influence of both locally produced O_3 and regional transport. The simulation of locally produced O_3 showed an increasing trend in spring, a decreasing trend in autumn, and no changes in summer and winter. The O_3 increase in spring was caused by the net effect of more rapid decrease in NO titration and unchanged TVOC reactivity despite decreased TVOC mixing ratios, while the decreased local O_3 formation in autumn was mainly due to the reduction of aromatic VOC mixing ratios and the TVOC reactivity and much slower decrease in NO titration. However, the decreased in situ O_3 formation in autumn was overridden by the regional contribution, resulting in elevated O_3 observations. Furthermore, the OBM-derived relative incremental reactivity indicated that the O_3 formation was VOC-limited in all seasons, and that the long-term O_3 formation was more sensitive to VOCs and less to NO_x and CO in the past 10 years. In addition, the OBM results found that the contributions of aromatics to O_3 formation decreased in all seasons of these years, particularly in autumn, probably due to the effective control of solvent-related sources. In contrast, the contributions of alkenes increased, suggesting a continuing need to reduce traffic emissions. The findings provide updated information on photochemical pollution and its impact in Hong Kong.

1 Introduction

Ozone (O_3), one of the most important photochemical products influencing atmospheric oxidative capacity, human and vegetation health, and climate change, is formed through a series of photochemical reactions among volatile organic compounds (VOCs) and nitrogen oxides (NO_x) in the atmosphere (Seinfeld and Pandis, 2006). Due to the non-linear relationship between O_3 and its precursors, the development of appropriate control measures for O_3 is still problematic in megacities (Sillman, 1999).

Distinguished from short-term O_3 studies, investigation of long-term O_3 variations enables us to understand the seasonal and inter-annual characteristics of O_3, the influence of meteorological parameters on O_3 formation, and the O_3–precursor relationships in different years. Subsequently, more effective and sustainable O_3 control strategies can be

formulated and implemented. Hence, earlier efforts have been made to investigate long-term variations of O_3 in different atmospheric conditions. For example, multi-year data analysis showed that O_3 levels started to decrease around 2000 in Europe (e.g. Jungfraujoch, Zugspitze, Mace Head) and North America excluding western US rural sites (e.g. US Pacific, Lassen Volcanic National Park; Lefohn et al., 2010; Cui et al., 2011; Parrish et al., 2012; Pollack et al., 2013; Lin et al., 2017), due to a decrease in the emissions of O_3 precursors since the early 1990s (Cui et al., 2011; Derwent et al., 2013). In contrast, the O_3 levels in East Asia increased at a rate of 1.0 ppbv yr^{-1} from 1998 to 2006, based on measurements at Mt Happo, Japan (Parrish et al., 2012; Tanimoto, 2009). In China, with rapid economic growth and urbanization over the past three decades, increasing O_3 levels have been found at many locations. For instance, based on the data collected between 1991 and 2006 at Lin'an, a NO_x-limited rural area close to Shanghai, Xu et al. (2008) reported that the maximum mixing ratios of O_3 increased by 2.0, 2.7, 2.4, and 2.0 % yr^{-1} in spring, summer, autumn, and winter, respectively, which were probably related to increased mixing ratios of NO_2. In the North China Plain (NCP), Ding et al. (2008) reported that O_3 in the lower troposphere over Beijing had a positive trend of $\sim$2.0 % yr^{-1} from 1995 to 2005, while Zhang et al. (2014) found that the daytime average O_3 in summer in Beijing significantly increased by 2.6 ppbv yr^{-1} from 2005 to 2011, due to decreased NO titration (-1.4 ppbv yr^{-1} of NO_x over the study period) and elevated regional background O_3 levels ($\sim$0.58–1.0 ppbv yr^{-1}) in the NCP.

Hong Kong, together with the inland Pearl River Delta (PRD) region of southern China, has suffered from high O_3 mixing ratios in recent years (Chan et al., 1998a, b; Wang and Kwok, 2003; Ding et al., 2004; Zhang et al., 2007; Guo et al., 2009, 2013). In 2014, O_3 exceeded the Chinese national air quality standard (80 ppbv, for the daily 8 h maximum average, DMA8) on more than 90 days in some areas of the PRD, with the highest DMA8 value of 165 ppbv (GDEMC and HKEPD, 2015). Based on the observational data at a newly established regional monitoring network, Li et al. (2014) found that O_3 mixing ratios in the inland PRD region increased at a rate of 0.86 ppbv yr^{-1} from 2006 to 2011 because of the rapid reduction of NO in this VOC-limited region. Similarly, Wang et al. (2009) reported a continuous record of increased surface O_3 at Hok Tsui (HT), a regional background site in Hong Kong, with a rate of 0.58 ppbv yr^{-1} based on observations conducted from 1994 to 2007, concluding that the increased NO_2 column concentration in upwind eastern China might significantly contribute to the increased O_3 in Hong Kong. Even so, knowledge gaps still exist regarding the long-term characteristics of O_3, long-term O_3–precursor relationships, and the mechanisms for the varying O_3 trends in the PRD region, because of the lack of long-term observations of VOCs in the region, where photochemical O_3 formation is sensitive to VOCs in urban areas, and where the levels of VOCs and NO_x have varied significantly due to more stringent control measures since 2005 (Zhong et al., 2013). It is noteworthy that although Xue et al. (2014) reported increasing O_3 trends in the period 2002–2013 in Hong Kong and investigated the roles of VOCs and NO_x in the long-term O_3 variations, only data from autumn were used, which could not provide a consistent and full picture of the long-term variations of O_3, VOCs, NO_x, and their relationships.

In this study, field measurements and model simulations were combined to characterize the long-term variations of O_3 and its precursors, the variations of locally produced O_3, and the impact of regional transport in Hong Kong from 2005 to 2014. In addition, the long-term contribution of different VOC groups to the O_3 formation was explored. The study aims to provide the most up-to-date information on the characteristics of photochemical pollution and its impact in Hong Kong.

2 Methodology

2.1 Site description

Field measurements were carried out at the Tung Chung (TC) Air Quality Monitoring Station managed by the Hong Kong Environmental Protection Department (HKEPD). The sampling site (22.29° N, 113.94° E) is located at about 24 km southwest of downtown Hong Kong and about 3 km south of Hong Kong International Airport (Fig. 1). The elevation of TC is 37.5 m above sea level. It is surrounded by a newly developed residential town on the northern Lantau Island, and is downwind of urban Hong Kong and the inland PRD region when easterly and northeasterly winds are prevailing (Ou et al., 2015). At TC, the prevailing wind varies by season, being from the east in spring and autumn, from the southwest in summer, and from the northeast in winter (see Fig. S1 in the Supplement). The selection of this site for the trend study was due to its downwind location being a good receptor for urban plume, suffering high O_3 pollution, and having the most comprehensive dataset. More detailed description of the TC site can be found in our previous papers (Jiang et al., 2010; Cheng et al., 2010; Ling et al., 2013; Ou et al., 2015).

2.2 Measurement techniques

Hourly observations of O_3, CO, SO_2, NO-NO_2-NO_x, and meteorological parameters at TC from 2005 to 2014 were obtained from the HKEPD (http://epic.epd.gov.hk/ca/uid/airdata). Briefly, O_3 was measured using a commercial UV photometric instrument (Advanced Pollution Instrumentation (API), model 400A) with a detection limit of 0.6 ppbv. CO was measured with a gas filter correlation CO analyser (Thermo Electron Corp. (TECO), model 48C) with a detection limit of 0.04 ppm. SO_2 was measured using a pulsed fluorescence analyser (TECO, model 43A) with a detec-

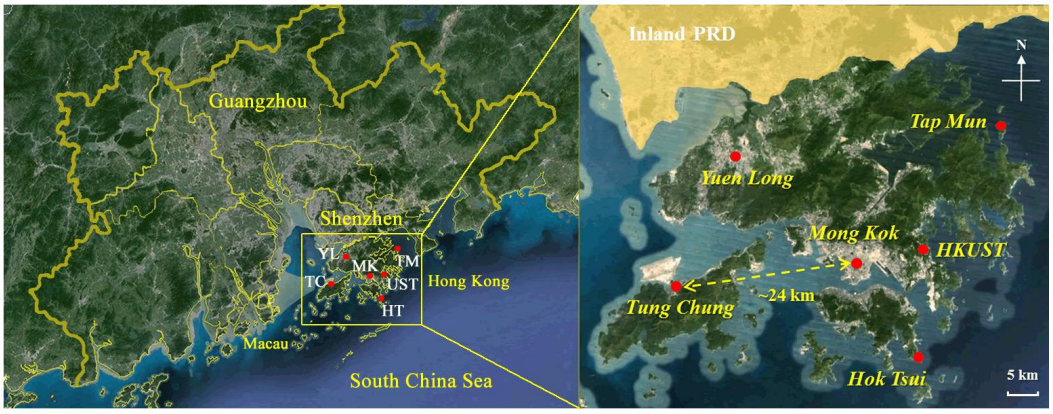

Figure 1. Location of the sampling sites and surrounding environments. Guangzhou and Shenzhen are the two biggest cities in the inland PRD region with a population of over 10 million for each city. Hok Tsui (HT) and Tap Mun (TM) are regional background sites. The Hong Kong University of Science and Technology (HKUST) is an Air Quality Research Supersite located in a suburban area. Yuen Long (YL) is a typical urban site adjacent to main traffic roads and surrounded by residential and industrial blocks. Mong Kok is a typical downtown roadside site with high traffic density.

tion limit of 1.0 ppbv. NO-NO_2-NO_x was detected using a commercial chemiluminescence with an internal molybdenum converter (API, model 200A) and a detection limit of 0.4 ppbv. All the time resolutions for these gas analysers are 1 h. To ensure a high degree of accuracy and precision, the QA/QC procedures for gaseous pollutants were identical to those in the US air quality monitoring programme (http://epic.epd.gov.hk/ca/uid/airdata). The accuracy of the monitoring network is assessed by performance audits, while the precision, a measure of the repeatability, of the measurements is checked in accordance with HKEPD's quality manuals. For the gaseous pollutants, accuracy and precision within the limits of ±15 and ±20 % are adopted, respectively (HKEPD, 2015).

Real-time VOC data at TC were also measured by the HKEPD. An online GC-FID analyser (Synspec GC 955, Series 600/800) was used to collect VOC speciation data continuously with a time resolution of 30 min. The VOC analyser consists of two separate systems for detection of C_2–C_5 and C_6–C_{10} hydrocarbons, respectively. Detailed description about the real-time VOC analyser can be found in Lyu et al. (2016). There were 28 C_3–C_{10} VOC species identified and quantified with this method. In terms of the QA/QC for VOC analysis, built-in computerized programmes of quality control systems such as auto-linearization and auto-calibration were used. Weekly calibrations were conducted by using NPL standard gas (National Physical Laboratory, Teddington, Middlesex, UK). In general, the detection limits of the target VOCs ranged from 2 to 56 pptv. The accuracy of each species measured by online GC-FID was determined by the percentage difference between measured mixing ratio and actual mixing ratio based on weekly span checks and monthly calibrations. The precision was based on the 95 % probability limits for the integrated precision check results. The accuracy of the measurements was about 1–7 %, depending on the species, and the measurement precision was about 1–10 % (Table S1 in the Supplement). In addition, the quality of the real-time data was assured by regular comparison with whole-air canister samples collected and analysed by the University of California at Irvine (UCI). More details can be found in reports of previous studies in Hong Kong (Xue et al., 2014; Ou et al., 2015; Lyu et al., 2016).

For data analysis, linear regression and error bars representing 95 % confidence intervals were used. Trends of O_3 and its precursors with a p value < 0.05 were considered significant (Guo et al., 2009).

2.3 Observation-based model

In this study, an observation-based box model (OBM) coupled with a carbon bond mechanism (CB05) was used to simulate photochemical O_3 formation and to evaluate the sensitivity of O_3 formation to its precursors. The CB05 mechanism is a condensed mechanism with high computational efficiency and reliable simulation, and has been successfully applied in many emission-based modelling systems such as Weather Research and Forecasting with Chemistry (WRF/Chem) and the Community Multiscale Air Quality (CMAQ; Yarwood et al., 2005; Coates and Butler, 2015). Unlike emission-based models, the OBM in this study is based on the real-time observations at the TC site in Hong Kong. The simulation was constrained by observed hourly data of meteorological parameters (temperature, relative humidity, and pressure) and air pollutants (NO, NO_2, CO, SO_2, and 22 C_3–C_{10} VOCs). In the CB05 module, VOCs are grouped according to carbon bond type and the reactions of individual VOCs were condensed using a lumped structure technique (conversions from measured VOCs to CB05 grouped species

are shown in Table S2). To better describe the photochemical reactions in Hong Kong, the photolysis rates of different species in the OBM were determined using the output of the Tropospheric Ultraviolet and Visible Radiation model (TUV v5; Madronich and Flocke, 1999) based on the actual conditions of Hong Kong, i.e. meteorological parameters, location, and time period of the field campaign. However, it is noteworthy that the atmospheric physical processes (i.e. vertical and horizontal transport), the deposition of species, and the radical loss to aerosol (George et al., 2013; Lakey et al., 2015) were not considered in the OBM. In addition, a "spin-up" time was not applied in the model to get the radical intermediates steady which might have caused a slight underestimation of the simulated O_3 production (Fig. S2) and its sensitivity to precursors (Fig. S3). In this study, we performed day-by-day OBM simulations for 2688 days during 2005–2014, where the missing days were due to lack of real-time VOC data (see Table S3). For each daily simulation, the model was run for a 24 h period with 00:00 (local time, LT) as the initial time. The model output simulated mixing ratios of O_3, radicals (i.e. OH, HO_2, RO, and RO_2), and intermediates. The model performance was evaluated using the index of agreement (IOA; Huang et al., 2005; Wang et al., 2015, 2013; Lyu et al., 2015a):

$$\mathrm{IOA} = 1 - \frac{\sum_{i=1}^{n}(O_i - S_i)^2}{\sum_{i=1}^{n}(|O_i - \overline{O}| + |S_i - \overline{O}|)^2}, \quad (1)$$

where S_i and O_i represent simulated and observed values, respectively, $\overline{O}$ represents the mean of observed values, and n is the number of samples. The IOA value lies between 0 and 1. The better the agreement between simulated results and observed data, the higher the IOA (Huang et al., 2005).

Apart from the OBM (CB05), which is mainly for condensed VOC groups, a Master Chemical Mechanism (MCM, v3.2) was applied to inter-compare the modelling performance of the OBM (CB05; shown in Sect. 3.2). Since the MCM utilizes the near-explicit mechanism describing the degradation of 143 primary VOCs and contains around 16 500 reactions involving 5900 chemical species, it has a better performance in calculating the contribution of individual VOCs to O_3 production (Jenkin et al., 1997, 2003; Saunders et al., 2003). The hourly input data of meteorological parameters, air pollutants, and the photolysis rates in MCM were the same as in CB05. It was assumed that the measured VOCs contributed a dominant fraction to O_3 production, and that the initial concentrations of those VOCs not measured but needed by MCM were zero. We acknowledge that the use of a limited number of VOCs causes some photochemical reactivity to be overlooked. For a more detailed description of the MCM, see Jenkin et al. (1997, 2003) and Saunders et al. (2003). Some developments on localization of the MCM for Hong Kong and the addition of chemical reaction pathways of more biogenic VOC species and alkyl nitrates are given in our previous papers (Lam et al., 2013; Cheng et al., 2013; Ling et al., 2014; Lyu et al., 2015b).

The measured precursors (i.e. VOCs, NO, and NO_2) at TC are a mixture of regional background values augmented by local source influences, and the two parts are very difficult to fully separate. It is worth noting that the regional background values are those observed at locations where there is little influence from urban sources of pollution, while the baseline values mentioned in Sect. 3.2 are observations made at a site not influenced by recent, locally emitted (or produced) pollution (TF HTAP, 2010). To minimize the influence of regional transport from the inland PRD region, the real-time regional background values in this study were simply subtracted from the observations at TC. Previous studies have reported that Tap Mun (TM; 22.47° N, 114.36° E) and Hok Tsui (HT; 22.217° N, 114.25° E) are two background sites of Hong Kong (Lyu et al., 2016; So and Wang, 2003, 2004; Wang et al., 2005, 2009). TM is a rural site that is upwind of Hong Kong in autumn/winter seasons and HT is a background site at the southeastern tip of Hong Kong. Good trace gas correlations have been found between the two sites (Lyu et al., 2016). Since not all the data during the entire 10-year period were available at one background site, the hourly measured VOCs at HT and NO_2 at TM were treated as background values. The background data were excluded using the following equations:

$$[\mathrm{VOC}]_{\mathrm{local}} = [\mathrm{VOC}]_{\mathrm{observed}} - [\mathrm{VOC}]_{\mathrm{background}}, \quad (2)$$

$$[\mathrm{NO}]_{\mathrm{local}} = [\mathrm{NO}]_{\mathrm{observed}} - [\mathrm{NO}]_{\mathrm{background}}, \quad (3)$$

$$[\mathrm{NO_2}]_{\mathrm{local}} = [\mathrm{NO_2}]_{\mathrm{observed}} - [\mathrm{NO_2}]_{\mathrm{background}}, \quad (4)$$

where $[xx]_{\mathrm{local}}$, $[xx]_{\mathrm{observed}}$, and $[xx]_{\mathrm{background}}$ represent the local, observed, and background values, respectively. In this study, mixing ratios of 21 anthropogenic VOC species with relatively long lifetimes (5 h–14 days) at HT were selected as the background values to deduct from the observed data at TC. The lifetimes of these VOCs were estimated based on the reactions with OH radicals (Simpson et al., 2010). The rate constants used were from Atkinson and Arey (2003) – assuming a 12 h daytime average OH radical concentration of 2.0×10^6 molecules cm^{-3}. Isoprene was considered as not having a regional impact due to its short lifetime (1–2 h; Ling et al., 2011). Furthermore, the lifetime of NO_2 is determined by the main sinks of OH+NO_2 reaction and the hydrolysis of N_2O_5 at the surface of wet aerosols, which highly depends on meteorological conditions, such as temperature and humidity (Dils, 2008; Evans and Jacob, 2005). Previous experimental studies showed an exponential relationship between the NO_2 lifetime and temperature (Dils, 2008; Merlaud et al., 2011; Rivera et al., 2013), which was used to estimate the lifetime of NO_2 in this study. The lifetime of NO_2 was calculated to be approximately 3.4 ± 0.3, 2.2 ± 0.1, 2.8 ± 0.2, and 5.2 ± 0.3 h in spring, summer, autumn, and winter, respectively, consistent with the lifetimes of NO_2 in different seasons in the PRD region (Beirle et al., 2011). Considering

the shortest distance between the inland PRD and TC (i.e. from the centre of Shenzhen to the TC site, ∼ 30 km) and the average wind speed in different seasons (Ou et al., 2015), it would take approximately 3.4 ± 0.3, 4.3 ± 0.3, 4.0 ± 0.5, and 3.7 ± 0.4 h in spring, summer, autumn, and winter, respectively, for NO_2 originating in the inland PRD to arrive at TC. Hence, although NO_2 emitted from the inland PRD is slightly more likely to arrive at TC in winter and spring than in summer and autumn, the differences in travel time between the seasons are relatively small and it is difficult to be precise about seasonal average estimates of NO_2 lifetime and travel time. We have excluded background NO_2 values in spring and winter in this study during model simulations, but we recognize the limitations in these calculations.

In addition to the simulation of O_3 formation, the precursor sensitivity of O_3 formation was assessed by the OBM using the relative incremental reactivity (RIR; Cardelino and Chameides, 1995; Lu et al., 2010; Cheng et al., 2010; Ling et al., 2011; Xue et al., 2014). A higher positive RIR of a given precursor means a greater probability that reducing emissions of this precursor will significantly reduce O_3 production. The RIR is defined as the percentage change in daytime O_3 production per percent change in precursor. The RIR for precursor X is given by

$$\mathrm{RIR}(X) = \frac{[\mathrm{P}^{\mathrm{S}}_{\mathrm{O_3-NO}}(X) - \mathrm{P}^{\mathrm{S}}_{\mathrm{O_3-NO}}(X - \Delta X)]/P^{\mathrm{S}}_{\mathrm{O_3-NO}}(X)}{\frac{\Delta S(X)}{S(X)}}, \quad (5)$$

where X represents a specific precursor (i.e. VOCs, NO_x, or CO); the superscript "S" is used to denote the specific site where the measurements were made; $S(X)$ is the measured mixing ratio of species X (ppbv); $\Delta S(X)$ is the hypothetical change in the mixing ratio of X; and $\mathrm{P}^{\mathrm{s}}_{\mathrm{O_3-NO}}(X)$ and $\mathrm{P}^{\mathrm{s}}_{\mathrm{O_3-NO}}(X - \Delta X)$ represent net O_3 production in a base run with original mixing ratios, and in a run with a hypothetical change ($\Delta S(X)$; 10 % $S(X)$ in this study) in species X. In both runs, O_3 production modulated by NO titration is considered during the evaluation period. The O_3 production $\mathrm{P}^{\mathrm{S}}_{\mathrm{O_3-NO}}$ was calculated by the output parameters of the OBM.

$\mathrm{P}^{\mathrm{S}}_{\mathrm{O_3-NO}}$ is derived from the difference between O_3 gross production rate $\mathrm{G}^{\mathrm{S}}_{\mathrm{O_3-NO}}$ and O_3 destruction rate $D^{\mathrm{S}}_{\mathrm{O_3-NO}}$ (Eq. 6). $\mathrm{G}^{\mathrm{S}}_{\mathrm{O_3-NO}}$ is calculated by the oxidation of NO by HO_2 and RO_2 (Eq. 7), while $D^{\mathrm{S}}_{\mathrm{O_3-NO}}$ is calculated by O_3 photolysis, reactions of O_3 with OH, HO_2 and alkenes, and reaction of NO_2 with OH (Eq. 8):

$$P^{\mathrm{S}}_{\mathrm{O_3-NO}} = G^{\mathrm{S}}_{\mathrm{O_3-NO}} - \mathrm{D}^{\mathrm{S}}_{\mathrm{O_3-NO}}, \quad (6)$$

$$\mathrm{G}^{\mathrm{S}}_{\mathrm{O_3-NO}} = k_{\mathrm{HO_2+NO}}[\mathrm{HO_2}][\mathrm{NO}] + \sum k_{\mathrm{RO_2}i+\mathrm{NO}}[\mathrm{RO_2}i][\mathrm{NO}], \quad (7)$$

$$\mathrm{D}^{\mathrm{S}}_{\mathrm{O_3-NO}} = k_{\mathrm{HO_2+O_3}}[\mathrm{HO_2}][\mathrm{O_3}] + k_{\mathrm{OH+O_3}}[\mathrm{OH}][\mathrm{O_3}] + k_{\mathrm{o(^1D)+H_2O}}[\mathrm{O(^1D)}][\mathrm{H_2O}] + k_{\mathrm{OH+NO_2}}[\mathrm{OH}][\mathrm{NO_2}] + k_{\mathrm{alkenes+O_3}}[\mathrm{alkenes}][\mathrm{O_3}]. \quad (8)$$

In Eqs. (7) and (8), k constants are the rate coefficients of their subscript reactions. Values of radicals and intermediates are simulated by the OBM. Details of the calculation can be found in Ling et al. (2014) and Xue et al. (2014).

Furthermore, the sensitivities in the OBM to the uncertainties in initial concentrations of O_3 precursors have been examined by running the model with varying NO_2 or VOCs initial concentrations in the range of ±95 % confidence intervals, respectively. The results demonstrate that the modelled O_3 production was more sensitive to NO_2 than VOCs, with a percentage variation about ±13 and ±3.9 %, respectively (see Table S4, Figs. S4 and S5). In addition, the uncertainties associated with removing the background concentrations are also evaluated, suggesting a similar trend for simulated local O_3 production for both approaches (see Fig. S6 and Tables S5–S7).

3 Results and discussion

3.1 Long-term trends of O_3 and its precursors

Figure 2 shows trends of monthly averaged mixing ratios of O_3 and its precursors, namely NO_x, total VOCs (TVOCs), and CO measured at TC in the past 10 years. Please note that arithmetic means were used here in order to compare with other studies. TVOC was defined as the sum of the 22 VOC species listed in Text S1. Note that not all detected VOCs were included in this study because of high rates of missing data. The limited number of VOC precursors causes a reduced reactivity which was estimated at < 30 % for total hydrocarbons based on our previous study (Guo et al., 2004). The missing reactivity would be larger if carbonyls were considered (Cheng et al., 2010). It was found that both monthly averaged O_3 and monthly maximum O_3 increased at a rate of 0.56 ± 0.01 ppbv yr^{-1} ($p < 0.01$) and 1.92 ± 0.15 ($p < 0.05$), respectively. The monthly maximum O_3 level, which was defined as the maximum of DMA8 O_3 in 1 month, increased from about 68 ppbv in 2005 to 86 ppbv in 2014, exceeding the ambient air quality standard in Hong Kong (i.e. 80 ppbv). The number of days per year (days yr^{-1}) that DMA8 exceeded 80 ppbv also increased during the period 2005–2014 (1.16 ± 0.26 days yr^{-1}, $p < 0.05$; see Fig. S7), indicating increasing O_3 pollution in Hong Kong. This finding is consistent with other big cities and regions in the world, such as Beijing (Tang et al., 2009), the West Plains of Taiwan (Chou et al., 2006), and Osaka (Itano et al., 2007). The annual average O_3 concentration in Hong Kong increased by 0.56 ppbv yr^{-1} in the period 2004–2015, which is close to that reported for Osaka (0.6 ppbv yr^{-1}) in the period 1985–2002, and in agreement with Lin et al. (2017),

who found that the annual mean O_3 over Hong Kong increased by about 0.5 ppbv yr^{-1} in the period 2000–2014. In contrast, NO_x and CO significantly decreased at an average rate of -0.71 ± 0.01 ($p < 0.01$) and -29.4 ± 0.05ppbv yr^{-1} ($p < 0.01$), respectively, while TVOC remained unchanged ($p = 0.71$) for these years. The decreasing trends of NO_x and CO, also observed in many other high-population industrial urban areas (Geddes et al., 2009; Tang et al., 2009), suggest effective reduction of local emissions from transportation, power plants, and other industrial activities (HKEPD, 2016). Unlike O_3 and NO_x, the trend of TVOC varied across different areas – for example, increasing in Beijing (Tang et al., 2009), decreasing in Toronto (Geddes et al., 2009) and Taiwan (Chou et al., 2006), while remaining almost unchanged ($p > 0.05$) in Hong Kong (Fig. 2). Although the 10-year TVOC trend did not change, their levels showed clear inter-annual variations in spring and autumn (Fig. 3). Moreover, the long-term trends of individual VOCs, except for BVOC, were different from that of TVOCs (see Fig. S8) because many control measures were taken in the last decade, which altered the composition of VOCs in the atmosphere, such as the reduction of toluene by solvent usage control and the increase in alkanes in liquefied petroleum gas (LPG) in 2005–2013 (Ou et al., 2015) and the decrease in LPG alkanes in 2013–2014 (Lyu et al., 2016).

Figure 3 displays variations of measured O_3 and its precursors (NO_x, TVOC, and CO) in four seasons in 2005–2014. Here we defined December–February, March–May, June–August, and September–November as winter, spring, summer, and autumn, respectively. Generally, all precursors showed low values in summer and high levels in winter, mainly due to typical Asian monsoon circulations, which brought in clean marine air in summer and delivered pollutant-laden air from mainland China in winter (Wang et al., 2009). A similar seasonal variation was observed for the TVOC averages at different locations over Hong Kong (see Table S8). With lower (diluted) precursor concentrations, together with a high frequency of rainy days, it is not uncommon for Hong Kong to see the lowest O_3 values in summertime (see Fig. 3).

The long-term trends of CO in all seasons (slopes from spring to winter: -39.2 ± 0.20, -16.8 ± 0.12, -14.4 ± 0.16, and -50.3 ± 0.23 ppbv yr^{-1}, respectively) and NO_x and TVOCs in spring (NO_x: -0.69 ± 0.01; TVOCs: -0.26 ± 0.01 ppbv yr^{-1}) and autumn (NO_x: -0.50 ± 0.02; TVOCs: -0.32 ± 0.01 ppbv yr^{-1}) showed significant decreases ($p < 0.05$), whereas NO_x and TVOCs did not have statistical variations in summer and winter during the 10 years ($p > 0.05$). The different inter-annual trends of NO_x and TVOCs in spring/autumn from those in summer/winter were probably because marine air significantly diluted air pollution in summer, while continental air masses remarkably burdened air pollution in winter, which concealed the decreased local emissions of NO_x and TVOCs in summer and winter (Wang et al., 2009). In

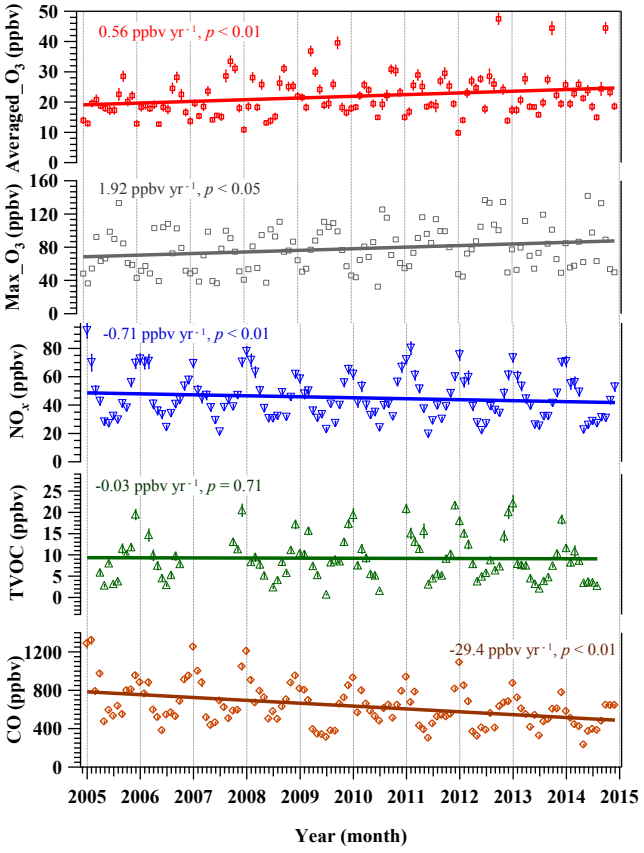

Figure 2. Trends of monthly averages of O_3 and its precursors, i.e. NO_x, TVOC, and CO at TC during 2005–2014. Error bars represent 95 % confidence intervals of monthly averages.

contrast, the measured O_3 trends significantly increased in spring, summer, and autumn, at the rate of 0.51 ± 0.05, 0.50 ± 0.04, and 0.67 ± 0.07 ppbv yr^{-1}, respectively ($p < 0.05$), while winter O_3 levels showed no significant trend (0.23 ± 0.05 ppbv yr^{-1}, $p = 0.11$). It is noteworthy that there were three extremely high O_3 data points in October months in the period 2012–2014 (Fig. 3), which seemed to bias the O_3 trend in autumn. However, it can be seen from Fig. S9, which shows the daily average O_3 values in autumn (i.e. more data points than in Fig. 3), that the values varied much more significantly in the period 2012–2014 than in previous years. It is worth emphasizing that the overall O_3 trend was determined by all the measured data points including both extremely high and low values in all the study years. Apart from the impact of regional transport, the increased spring and autumn O_3 in these years was probably due to the reduction of NO titration overriding the O_3 decrease owing to the reduction of TVOCs, leading to a net O_3 increase. Here the NO titration refers to the "titration reaction" between NO and O_3. Although NO–NO_2–O_3 reaction cycling (including the effects of NO titration; see Reactions R1–R3) can be theoretically regarded as a null

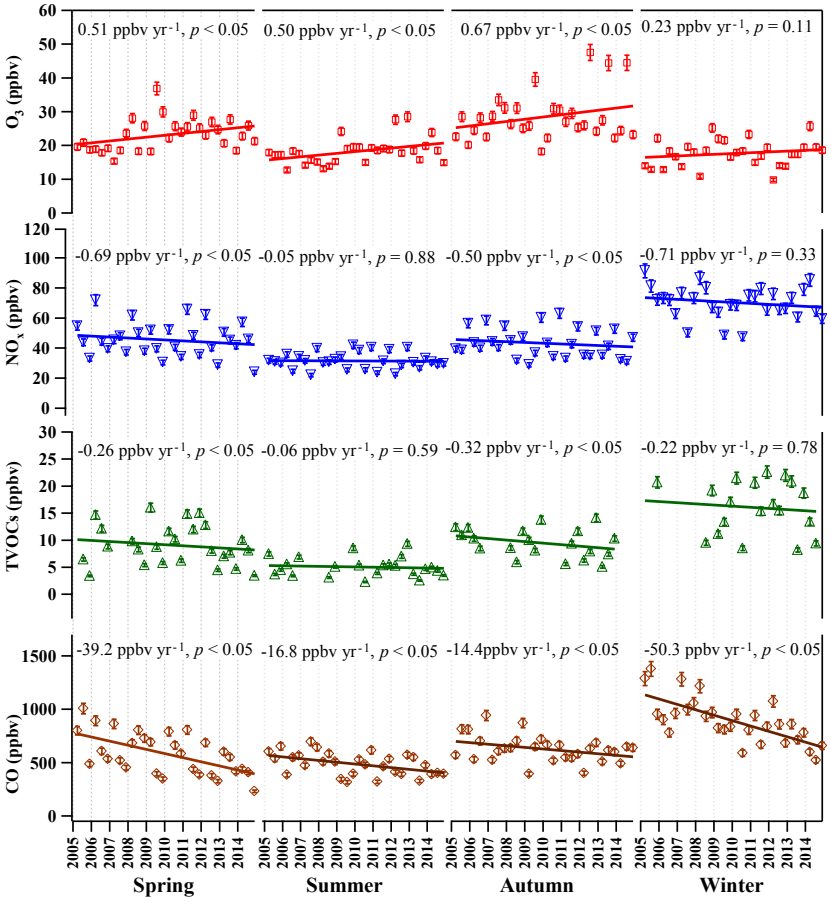

Figure 3. Variations of O_3 and its precursors in four seasons at TC during 2005–2014. Each data point in the figure is obtained by averaging hourly values into a monthly value. Error bars represent 95 % confidence intervals of the averages. In the sub-plot for O_3 trend in autumn, the three extremely high values are not considered as outliers as each of them represents 1 month of data with relatively small uncertainty (see Fig. S9).

cycle and provides rapid cycling between NO and NO_2, the NO titration effect can retard the accumulation of O_3 in an urban environment by means of substantial NO emissions (Chou et al., 2006). Indeed, the observed NO at TC site decreased significantly during the 2005–2010 period (shown in Fig. S10), which mitigated the effects of NO titration and led to the increase in O_3:

$$NO_2 + h\nu \rightarrow NO + O, \quad \text{(R1)}$$

$$O + O_2 + M \rightarrow O_3 + M, \quad \text{(R2)}$$

$$NO + O_3 \rightarrow NO_2 + O_2. \quad \text{(R3)}$$

Interestingly, summer O_3 significantly increased although NO_x and TVOCs showed no differences in these years. Further investigation found that temperature and solar radiation in summer increased ($p < 0.05$) in these years (see Fig. S11), whereas they had no significant change in other seasons (the reasons remain unclear), consistent with the fact that an increase in temperature and solar radiation would enhance the photochemical reaction rates, resulting in O_3 increase in summer (Lee et al., 2014). On the other hand, the unchanged winter O_3 trend was in line with the unchanged NO_x and TVOC values in winters of the past 10 years. Again, the impact of regional transport could not be ignored. To better understand the mechanisms of long-term trends of O_3 in different seasons in this study, the source origins of O_3, i.e. whether it was locally formed or transported from other regions, were explored.

3.2 Long-term trends of locally produced O_3 and regional contribution

In this study, the OBM (CB05) was used to simulate the long-term trends of O_3 produced by in situ photochemical reactions – hereinafter locally produced O_3 (simulated). The comparisons of simulated and observed O_3 at TC during the period 2005–2014 are shown in Figs. S12 (by year) and S13 (by month); Table S9 lists the IOA values between observed and locally produced O_3 (simulated) at TC site in each year. As shown, the IOA values range from 0.71 to 0.89, indicating

that the performance of the OBM in the O_3 simulation was acceptable.

It is noteworthy that MCM has better simulation performance than CB05 due to its near-explicit rather than condensed chemical mechanism. Indeed, the overall IOA of MCM modelling (0.89) was higher than that of CB05 (0.81), according to our test on the same sampling days of 2005–2014 (shown in Fig. S14; rainy days were excluded). Despite this, the high computational efficiency OBM (CB05) was used for the 10-year day-by-day O_3 simulations to investigate the long-term trend of O_3 in this study, because the simulated results of both CB05 and MCM models followed similar temporal patterns ($p > 0.05$), and the difference of simulated values between the two models was reasonable (IOA value: 0.89 vs. 0.81), revealing that the condensed mechanism of CB05 would not significantly affect the long-term trends of O_3 in this study (shown in Fig. S15).

Previous studies suggest that a wind speed of $2\,m\,s^{-1}$ could be used as a threshold to classify regional and local air masses in Hong Kong (Guo et al., 2013; Ou et al., 2015; Cheung et al., 2014). That is, the O_3 values measured with $< 2\,m\,s^{-1}$ in this study were considered as locally produced O_3 – hereinafter locally produced O_3 (filtered). Figure 4 presents the long-term trends of observed daytime O_3 (07:00–19:00 LT) and locally produced O_3 (filtered/simulated) in four seasons during the period 2005–2014. Although the actual duration of daytime in Hong Kong varies by 1–2 h according to season, the expected uncertainty from it would be limited when considering weak photochemical reactions in the early morning and in the late afternoon. Also note that the trends of observed daytime O_3 in the four seasons were consistent with those of 24 h observed O_3 (see Fig. S16). It can be seen that the locally produced O_3 (simulated) increased in spring (0.28 ± 0.01 ppbv yr^{-1}, $p < 0.05$), decreased in autumn (-0.39 ± 0.02 ppbv yr^{-1}, $p < 0.05$), and showed no change in summer and winter ($p > 0.05$). Interestingly, the long-term trend of locally produced O_3 (simulated) in autumn was opposite to that in spring although both NO_x and TVOCs decreased in the two seasons. The reasons were because (1) NO_x decreased faster while TVOCs decreased more slowly (Fig. 3) in spring than in autumn, leading to a net increase in O_3 formation in spring and a decrease in autumn, and (2) TVOC reactivity (described in Text S2 and Table S10) decreased in autumn ($-0.03\,s^{-1}\,yr^{-1}$, $p < 0.05$) but showed insignificant variations in other seasons ($p > 0.1$; Fig. S17), resulting in the reduction of O_3 production in autumn. The simulated springtime O_3 increase and unchanged winter values were consistent with the observed trends, whereas the simulated autumn O_3 decrease was opposite to the observed trend for the overall observations. However, locally produced O_3 (filtered) values clearly showed similar trends to locally produced O_3 (simulated) in spring, autumn, and winter (see Fig. 4), confirming that locally produced O_3 indeed increased in spring and decreased in autumn in these years.

In comparison, a significant difference ($\Delta O_3 = O_3$ $overall_{observed} - O_{3\,simulated}$, $p < 0.01$) was found between measured and simulated O_3 in spring, implying the contribution of regional transport to the measured O_3. The 10-year average ΔO_3 was 8.26 ± 1.77 ppbv and the long-term trend of ΔO_3 showed no significant change ($p = 0.91$), suggesting that the contribution of regional transport in spring has been stable during the last decade. The spring pattern of O_3 in this study is consistent with the findings of Li et al. (2014), who reported the increasing O_3 trend (2.0 ppbv yr^{-1}) in spring at urban clusters of PRD from 2006 to 2011. In conclusion, the increasing O_3 trend in spring at TC was caused by the increased local O_3 production, and the contribution of regional transport was steady in the 2005–2014 period.

Unlike in spring, though the observed and locally produced O_3 (filtered) displayed increasing trends in summer (0.67 ± 0.34 and 0.61 ± 0.41 ppbv yr^{-1}, respectively; $p < 0.05$), locally produced O_3 (simulated) showed no significant change ($p = 0.18$), consistent with the unchanged trends of precursors (NO_x and TVOCs) in summer (Fig. 3). Note that the influence of annual variation in solar radiation over the 10 years was not considered while the TUV model was used to calculate the photolysis rates, which could mask the actual trends of O_3 mixing ratios. Indeed, the total solar radiation ($0.24 \pm 0.16\,MJ\,m^{-2}\,yr^{-1}$, $p < 0.01$) and temperature ($0.095 \pm 0.034\,K\,yr^{-1}$, $p < 0.05$) in summer significantly increased during the past 10 years (see Fig. S11), subsequently resulting in the enhanced in situ photochemical reactivity of VOCs, although their quantitative contributions remain unknown and require further investigation. The increase in solar radiation might be due to the decreasing haze as the air quality has been getting better in Hong Kong and the PRD (Louie et al., 2013). Moreover, the summertime wind speeds significantly decreased at a rate of $-0.062 \pm 0.041\,m\,s^{-1}\,yr^{-1}$ ($p < 0.05$), which might contribute to accumulation of the locally produced O_3. Lastly, the locally produced O_3 (filtered) trend was comparable to observed O_3 ($p = 0.12$) and locally produced O_3 (simulated; $p = 0.32$), indicating a negligible impact of regional transport on the summer O_3 trend in the period 2005–2014 (and thereby ΔO_3 in summer, not shown in Fig. 4). As such, the increasing trend of summer O_3 was partly attributed to the increase in solar radiation and temperature from 2005 to 2014.

Consistent with the decreasing trends of NO_x and TVOCs in autumn, both locally produced O_3 (simulated; $p < 0.05$) and locally produced O_3 (filtered; $p < 0.1$) remarkably decreased, suggesting the dominant impact of VOC reduction over the reduction of NO titration. The decreased locally produced O_3 in autumn was consistent with the results of Xue et al. (2014), who found that local O_3 production decreased in autumn from 2002 to 2013. Furthermore, the 10-year average ΔO_3 was 7.35 ± 3.16 ppbv and the long-term trend of ΔO_3 increased at a rate of 1.09 ± 0.21 ppbv yr^{-1} ($p < 0.05$), suggesting an increased contribution of regional transport in autumn during the last decade, in line with the fact that au-

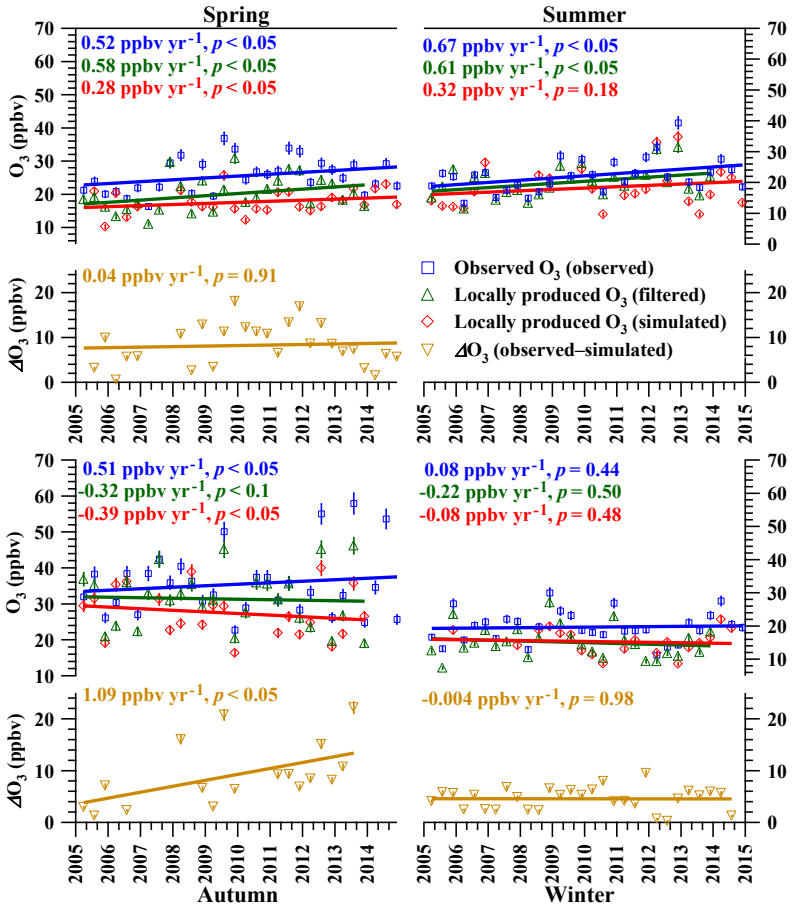

Figure 4. Trends of locally produced O_3 simulated by OBM (red line), observed O_3 (blue line: overall observed O_3; green line: locally produced O_3 (filtered), i.e. observed O_3 with hourly wind speed $< 2\,m\,s^{-1}$), and regional O_3 (gold line, $\Delta O_3 = O_3$ overall observed – O_3 simulated) in four seasons at TC during the period 2005–2014. Note: all the data are based on daytime hours (07:00–19:00 LT). The regional O_3 in summer was negligible and is not shown in the graph. Error bars represent 95 % confidence intervals of the averages.

tumn O_3 level in inland PRD was higher and increased more rapidly than in Hong Kong (Fig. 5), and high O_3 mixing ratios were frequently observed in this season due to stronger solar radiation, lower wind speeds, and less vertical dilution of air pollution than in other seasons in this region. In summary, locally produced O_3 in autumn decreased due to the reduction of dominant VOC precursors, while an increased contribution of regional transport negated the local reduction, leading to an elevated O_3 observation.

In winter, locally produced O_3 (filtered and simulated) had similar trends ($p = 0.93$) and the trends showed no significant changes ($p > 0.05$), confirming similar locally produced O_3 in these years, due to insignificant variations of NO_x and TVOCs levels (Fig. 3). Also, locally produced O_3 (both filtered and simulated) presented significant differences from the observed O_3 ($p < 0.01$), implying a regional contribution in winter. The 10-year average ΔO_3 was 4.56 ± 0.78 ppbv and the long-term trend of ΔO_3 was not significant ($p = 0.98$).

To further investigate the regional transport from the PRD region to Hong Kong, the observed O_3 values at PRD sites and at TC site in four seasons between 2006 and 2014 are compared (Fig. 5). Generally, the observed O_3 levels in PRD were all higher than those at TC in the four seasons ($p < 0.05$). Considering that the PRD is upwind of Hong Kong in spring/autumn/winter (Ou et al., 2015), high O_3-laden air in the PRD region could transport to Hong Kong in these three seasons. Moreover, comparable long-term trends were found between the sites in PRD and the TC site in spring (PRD: 0.49 ± 0.06; TC: 0.51 ± 0.05 ppbv yr^{-1}) and winter (PRD: 0.30 ± 0.06; TC: 0.23 ± 0.05 ppbv yr^{-1}), indicating that regional transport in spring and winter was stable in these years. In comparison, autumn O_3 level in inland PRD increased (0.84 ± 0.08 ppbv yr^{-1}) more rapidly than in Hong Kong (0.67 ± 0.07 ppbv yr^{-1}), implying an elevated regional contribution to Hong Kong. Therefore, the differences of observed O_3 between PRD and TC in spring/autumn/winter were consistent with the above calculations of average ΔO_3, confirming regional contribution to the observed O_3 in Hong

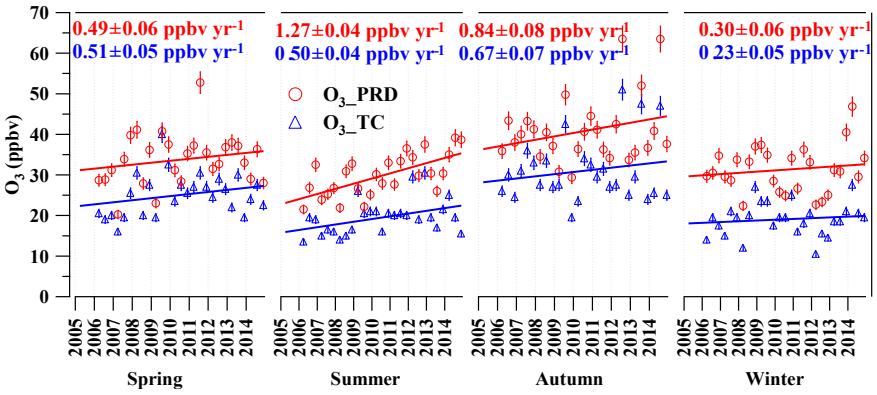

Figure 5. Trends of observed O_3 in inland PRD (red line) and at TC (blue line) in four seasons during the period 2006–2014. Each data point in the figure is obtained by averaging hourly values into a monthly value. Note: due to the location of sites which might have O_3 transport to TC (Guo et al., 2009), three regional background sites (i.e. Wanqingsha, Jinguowan, and Tianhu) and an urban site (i.e. Haogang) in Dongguan are used for comparison. Error bars represent 95 % confidence interval of monthly averages.

Kong. In contrast, though the increasing rate of O_3 level in PRD was much faster than at TC in summer, the impact of regional transport from the PRD region was insignificant due to the dominance of southerly and southwesterly winds from the South China Sea.

Overall, locally produced O_3 (simulated) in Hong Kong varied by season, showing an increase in spring, a decrease in autumn, and no change in summer and winter. The elevated observed O_3 in spring/summer/autumn was mainly attributed to the increase in locally produced springtime O_3 and constant regional contribution, increased summertime in situ photochemical reactivity, and regional contribution in autumn. Moreover, since the NO_x and NO levels significantly decreased during the last decade (Fig. S10), the reduced effect of NO titration, to a certain extent, made contribution to local O_3 levels. The effect of NO titration has also been reported in other areas (i.e. Beijing, Taiwan, Guangdong Province in China, and Osaka in Japan; Chou et al., 2006; Itano et al., 2007; Tang et al., 2009; Li et al., 2014). To confirm the reduction of NO titration in this study, the variation of O_x, the total oxidant estimated by O_3+NO_2 was investigated. According to the reaction of NO titration ($NO+O_3 \rightarrow NO_2+O_2$), the sum of O_3 and NO_2 (i.e. total oxidant O_x) remained essentially constant regardless the variation of NO (Chou et al., 2006). Indeed, the mixing ratio of local O_x (filtered by wind speed $< 2\,m\,s^{-1}$) showed no significant change ($p = 0.42$) at TC site, during the period 2005–2013 (Fig. 6), suggesting that the increase in O_3 was a result of the reduced NO titration. The reduction of NO titration was also confirmed by the increasing NO_2 / NO_x ratio at a roadside site (Mong Kok) in Hong Kong. The NO_2 / NO_x emission ratio is a parameter that can be used to examine the variation of NO titration (Carslaw, 2005; Yao et al., 2005; Dallmann et al., 2011; Tian et al., 2011; Ning et al., 2012; Lau et al., 2015). Generally, higher ratios of NO_2 / NO_x mean a lower potential of O_3 titration by NO, resulting in higher O_3. Indeed, the NO_2 / NO_x ratio at Mong Kok significantly increased, with enhanced traffic-related NO_2 / NO_x ratios observed at night, from 2005 to 2014 ($p < 0.01$), leading to increased local O_3 levels (Fig. 7). This finding was supported by the Hong Kong emission inventory, which indicated that the NO_x emission decreased from 1997 to 2014 in Hong Kong (HKEPD, 2016), and studies conducted by Tian et al. (2011) and Lau et al. (2015), who found an increasing trend of primary NO_2 emission in Hong Kong due to several diesel retrofit programmes in the period 1998–2008.

Apart from the regional and local impact on O_3 trends, the impact of variations of baseline O_3 was also considered. Oltmans et al. (2013) reported that O_3 at mid-latitudes of the Northern Hemisphere was flat or declining during the period 1996–2010 and the limited data in the subtropical Pacific suggested very little change during the same period. Thus, the O_3 trend in Hong Kong might be unaffected or underestimated given the flatness or decline of baseline O_3. Therefore, the increasing trend of O_3 in Hong Kong over the last decade was the integrated influence of its precursors, meteorological parameters, and regional transport.

3.3 Ozone–precursor relationships

Ozone–precursor relationships are critical to determine the reduction plan of precursors for future O_3 control. In this study, the RIR of major O_3 precursors was calculated by the OBM, to directly reflect the O_3 alteration in response to the percentage changes of its precursors (see Sect. 2.3). Furthermore, the long-term trend of RIR was used to evaluate the variation of the sensitivity of O_3 formation to each individual precursor. Figure 8a shows the average RIR values of O_3 precursors in the four seasons during the last decade. The RIR values of TVOCs (AVOC + BVOC, where AVOC means anthropogenic VOC and BVOC means biogenic VOC; see Sect. 3.4 for the definition of BVOC) ranged from

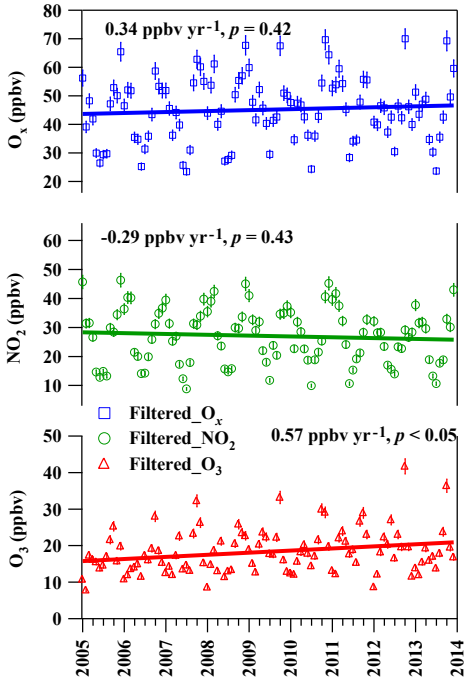

Figure 6. Annual trend of O_x, O_3, and NO_2 (filtered) at TC in the period 2005–2013. Error bars represent the 95 % confidence intervals of the averages.

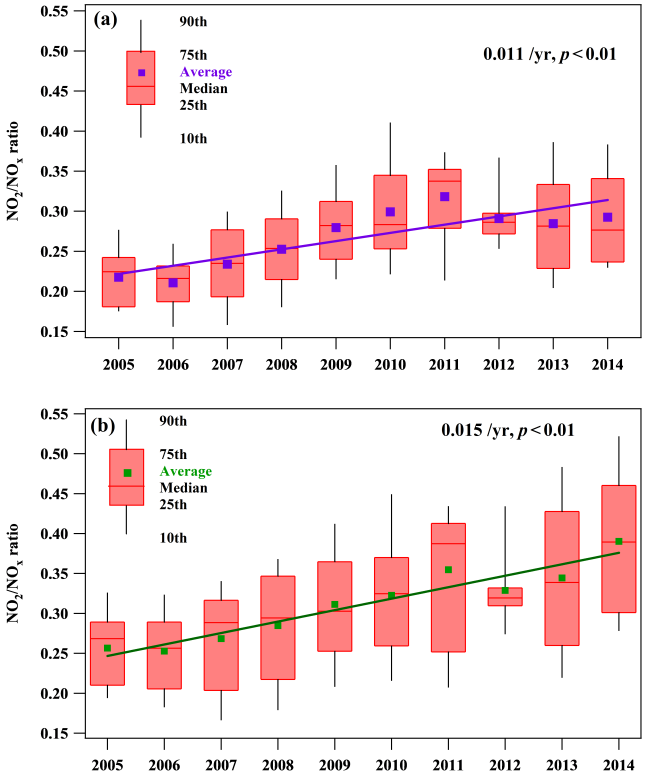

Figure 7. Annual trend of monthly average NO_2 / NO_x ratio at MK site in daytime **(a)** and night-time **(b)** in Hong Kong in the period 2005–2014. Hourly observations of NO_2 and NO_x are obtained at MK from the HKEPD (http://epic.epd.gov.hk/ca/uid/airdata). Note that data of October in 2014 are excluded due to the impact of Occupy Central event in Hong Kong.

0.78 ± 0.04 to 0.89 ± 0.04, followed by CO (0.32 ± 0.01 to 0.37 ± 0.01) in all seasons, suggesting the dominant role of TVOCs in photochemical O_3 formation. Among TVOCs, AVOCs had their highest RIR value in winter (0.80 ± 0.03, $p < 0.05$) and lowest in summer (0.39 ± 0.02, $p < 0.05$). Since RIR values are highly dependent on precursor mixing ratios (Eq. 5), the difference of RIR values of AVOCs in the four seasons was mainly caused by seasonal variations of observed AVOC levels (Fig. 3). In contrast, BVOCs had the highest RIR in summer (0.47 ± 0.02, $p < 0.05$), followed by autumn, spring, and winter (0.30 ± 0.02, 0.28 ± 0.02, and 0.09 ± 0.01, respectively). The higher RIR of BVOCs in summer was mainly due to the higher biogenic emissions in summer. In addition, higher photochemical reactivity of BVOCs also contributed to higher RIR of BVOCs (Atkinson and Arey, 2003; Tsui et al., 2009). The RIR values of NO_x, in contrast, were negative in all seasons, indicating that reducing NO_x would lead to an increase in photochemical O_3 formation. The RIR values of NO_x were lower in spring (-1.15 ± 0.02) and summer (-1.22 ± 0.02) than in autumn (-1.05 ± 0.02) and winter (-1.00 ± 0.01, $p < 0.05$), suggesting that reducing NO_x would increase more O_3 in spring and summer. The aforementioned findings were consistent with the results of previous studies conducted in autumn in Hong Kong, which were based on modelled and observed VOC / NO_x ratios (Zhang et al., 2007; Cheng et al., 2010; Ling et al., 2013; Guo et al., 2013). The relationship analyses suggest that the O_3 formation in Hong Kong was VOC-limited in all seasons in these years; that is, the O_3 formation was dominated by AVOCs in winter and was sensitive to both AVOCs and BVOCs in the other three seasons, whereas reducing NO_x emissions enhanced O_3 formation – the more so in spring and summer. The findings suggest that a simultaneous cut of AVOCs and NO_x (which is often the case in real situations) would be most effective in O_3 pollution control in winter, but least efficient in summer.

Figure 8b presents the long-term trends of RIR values of O_3 precursors from 2005 to 2014. The RIR values of TVOCs and NO_x increased at an average rate of 0.014 ± 0.012 ($p < 0.05$) and $0.009 \pm 0.01\ \mathrm{yr}^{-1}$ ($p < 0.05$), respectively, while the RIR of CO decreased at an average rate of $-0.014 \pm 0.007\ \mathrm{yr}^{-1}$ ($p < 0.01$). The evolution of RIR values suggested that the O_3 formation was more sensitive to TVOCs and less to CO and NO_x, indicating that VOCs reduction strategies would be more effective at O_3 control. The decreasing sensitivities of O_3 formation to both CO and NO_x were consistent with the decrease in their mixing ratios during the last decade. The sensitivity of O_3 formation to TVOCs increased although the 10-year levels of TVOCs

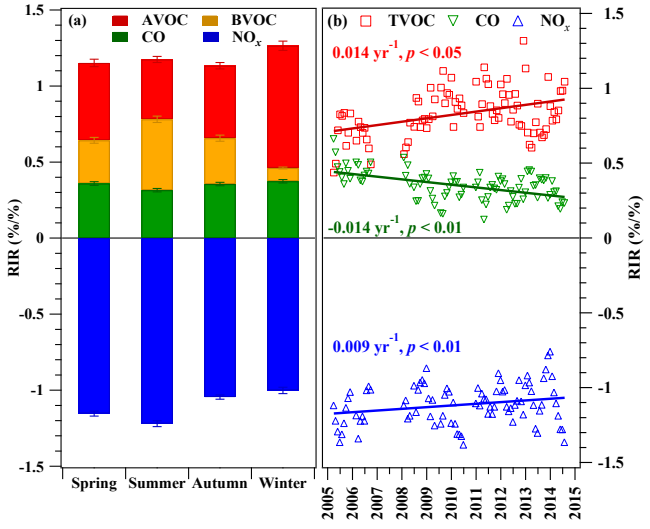

Figure 8. **(a)** Average RIR values of O_3 precursors in the four seasons and **(b)** trends of RIR values of O_3 precursors at TC from 2005 to 2014. AVOC represents anthropogenic VOCs, including 20 VOC species. BVOC means biogenic VOCs, including isoprene. Note: all the data are based on daytime hours (07:00–19:00 LT).

showed no significant trend, which might be attributed to the variations of speciated VOC levels and the VOC / NO_x ratios in these years (Ou et al., 2015). Furthermore, the monthly variation of TVOC / NO_x ratios showed a statistically significant decreasing trend at a rate of $-0.02\,yr^{-1}$ ($p < 0.05$; see Fig. S18). The weak declining trend moderately supports the view that VOC reduction has become more effective in reducing O_3 in the past 10 years, which is consistent with the conclusions from the above modelling results.

3.4 Contribution of VOC groups to O_3 formation

Since the local O_3 production was VOC-limited in Hong Kong, it is important to study the contribution of VOC species to the O_3 formation. To facilitate analysis and interpretation, AVOC species were categorized into three groups – namely, AVOC (aromatics; including benzene, toluene, m/o-xylenes, ethylbenzene, and three trimethylbenzene isomers), AVOC (alkenes; including propene, three butene isomers, and 1,3-butadiene), and AVOC (alkanes; including propane, n/i-butanes, n/i-pentanes, n/i-hexanes, and n-heptane). It is noteworthy that C_2 hydrocarbons were not included in the groups due to high missing rates of the C_2 data. The variations of the daytime averaged contributions of the four VOC groups (i.e. AVOC (alkanes/alkenes/aromatics) and BVOC) to O_3 mixing ratios were calculated by OBM and are shown in Fig. 9. Two scenarios were selected for data analysis. The first scenario was "origin", which used all originally measured data as input. The second scenario was "AVOC (aromatics/alkenes/alkanes) or BVOC group", which excluded each of the four VOC groups in turn from the input data in the

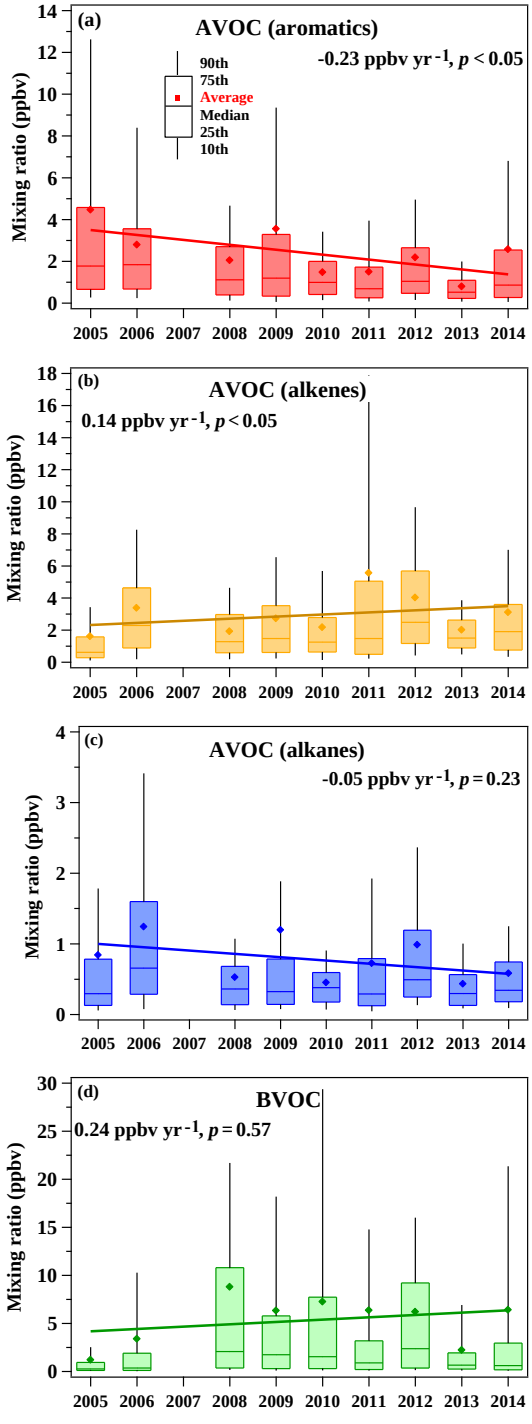

Figure 9. Trends of the daytime averaged contribution of four VOC groups to O_3 mixing ratio: **(a)** AVOC (aromatics), **(b)** AVOC (alkenes), **(c)** AVOC (alkanes), and **(d)** BVOC at TC during the period 2005–2014.

"origin" scenario. Hence, the contributions of VOC groups ((AVOC (aromatics/alkenes/alkanes) and BVOC) were obtained from the difference of simulated O_3 between the scenario "origin" and the related "VOCs group (AVOC (aromatics/alkenes/alkanes) or BVOC))". Clearly, the contribution of AVOC (aromatics) to O_3 mixing ratios significantly decreased at an average rate of -0.23 ± 0.01 ppbv yr^{-1} ($p < 0.05$), while AVOC (alkenes) made increasing contribution to O_3 mixing ratio ($p < 0.05$). BVOC and AVOC (alkanes) showed no significant changes ($p > 0.05$). The decreased contribution of AVOC (aromatics) to the O_3 mixing ratio was probably due to the decrease in C_6–C_8 aromatics, consistent with previous studies which found that aromatic levels decreased during the period 2005–2013 in Hong Kong (Ou et al., 2015). In fact, the Hong Kong Government has implemented a series of VOC-control measures since 2007 (HKEPD, 2016). In April 2007, the Air Pollution Control (VOCs) Regulation was implemented to control VOC emissions from regulated products, including architectural paints/coatings, printing inks, and six selected categories of consumer products. In January 2010, the regulation was extended to other high VOC-containing products, namely vehicle refinishing paints/coatings, vessel and pleasure craft paints/coatings, adhesives and sealants. The reduced contribution of AVOC (aromatics) to O_3 formation in these years also agreed well with the decreasing O_3 production rate of aromatics in autumn at TC from 2002 to 2013 reported by Xue et al. (2014). Furthermore, source apportionment results from Lyu et al. (2017) showed that solvent-related VOCs decreased at a rate of 204.7 ± 39.7 pptv yr^{-1} at the TC site, confirming that the reduction of solvent usage in these years was effective in decreasing the contribution of aromatics to O_3 production.

In contrast, the contributions of AVOC (alkenes) to O_3 production in these years showed a significant increasing trend with a rate of 0.14 ± 0.01 ppbv yr^{-1} ($p < 0.05$), perhaps attributed to the increased emissions of alkenes from changes in the composition of the traffic fleet and from increased traffic volume. During the period 2005–2014, the Hong Kong government launched a series of measures to reduce vehicular emissions, including diesel, LPG, and gasoline vehicles (http://www.epd.gov.hk/epd/english/environmentinhk/air/prob_solutions/air_problems.html).
Among the measures, gasoline and LPG vehicular emissions caused ambient alkenes to increase during the same period due to the increasing number of LPG/gasoline vehicles and some short-term/non-mandatory measures (Lyu et al., 2017). The diesel commercial vehicle (DCV) programme (2007–2013) was shown to be effective in reducing the emission of alkenes from diesel vehicles (Lyu et al., 2017). However, these vehicles emit significantly lower level of VOCs than gasoline-propelled vehicles. In consequence, the overall emissions of alkenes from traffic-related sources increased during the period 2005–2014, leading to the increased contribution of AVOC (alkenes) to O_3 formation (Lyu et al., 2017).

Unlike AVOC (aromatics/alkenes), the contribution of AVOC (alkanes) to O_3 formation during the period 2005–2014 showed no significant change ($p = 0.23$) despite the increase in total alkane levels in the atmosphere in the 2005–2013 period (Ou et al., 2015). This is because alkanes include a number of compounds which have different but generally low reactivity with OH radicals. Hence, although the level of total alkanes increased over the years, it did not cause an increase in its contribution to O_3 formation. For example, one possible case is that some alkanes with relatively high reactivity decreased, offset by an increase in some low-reactivity alkanes. In addition, the seasonal variation of O_3 formation, of which the reaction rate of alkanes with OH radicals was high in summer and low in winter, would also blur the trend.

Furthermore, BVOC showed no evident change in its contribution to O_3 mixing ratios during the last decade ($p = 0.57$), which is probably attributable to the lack of significant change of isoprene levels at the TC site during the 2005–2014 period (shown in Fig. S8). In this study, isoprene is defined as a biogenic VOC. The main known sources of isoprene are biogenic and anthropogenic (Borbon et al., 2001; Barletta et al., 2002; Reiman et al., 2000). It is noteworthy that according to the tunnel study in Hong Kong (Ho et al., 2009), vehicular emissions of isoprene are not significant in this city. Another tunnel study in the PRD region (Tsai et al., 2006) found that isoprene was not present in diesel-fuelled vehicular emissions in Hong Kong, probably related to variations in fuel type and vehicular engines used in different countries (Ho et al., 2009). In addition, in low-latitude areas like Hong Kong, with a high level of plant coverage (more than 70 %), isoprene is mainly produced by biogenic emissions. The source of isoprene at the TC site has been also investigated and confirmed by previous long-term source apportionment studies, which reported that during the period 2005–2013 about 90 % of isoprene was from biogenic emissions, with minor contribution from traffic emissions, consumer products, and printing processes (Ou et al., 2015). Therefore, in this study the traffic source of isoprene in Hong Kong was disregarded and isoprene was defined as a biogenic VOC.

4 Conclusions

In this study, the long-term trends of O_3 and its precursors (NO_x, TVOCs and CO) were analysed at TC from 2005 to 2014. It was found that NO_x and CO decreased while TVOCs remained unchanged, suggesting the effective reduction of some emissions in Hong Kong. However, ambient O_3 levels increased in these years and the locally produced O_3 showed different variations in the four seasons, reflecting the complexity of photochemical pollution in Hong Kong. To effectively control locally produced O_3, VOC control plays a vi-

tal role, since O_3 formation in Hong Kong was shown to be VOC-limited in these years. Moreover, trend studies found that the sensitivity of O_3 formation gradually increased with VOCs and decreased with NO_x and CO, indicating that controlling VOCs will be increasingly effective for O_3 control in the future. Among the VOCs, the contribution of aromatics to O_3 formation decreased in the period 2005–2014, consistent with their declining abundance over this period and implying effective control measures of solvent-related sources. In contrast, the contribution of anthropogenic alkenes increased, suggesting a continuing need for the control of traffic-related sources. In addition, of the four seasons, the highest sensitivity of O_3 formation to AVOC and the relatively low sensitivity to NO_x concurrently appeared in winter, suggesting that winter is the best time for O_3 control. Lastly, in addition to locally produced O_3, regional transport of O_3 from the PRD region made a substantial contribution to ambient O_3 in Hong Kong and even increased in autumn. In the future, the Hong Kong government should collaborate closely with Guangdong Province to mitigate O_3 pollution in this region.

Data availability. The data used in this study are not publicly accessible due to the privacy restrictions of HKEPD.

The Supplement related to this article is available online at https://doi.org/10.5194/acp-17-10919-2017-supplement.

Competing interests. The authors declare that they have no conflict of interest.

Disclaimer. The opinions expressed in this paper are those of the authors and do not necessarily reflect the views or policies of the government of the Hong Kong Special Administrative Region, nor does the mention of trade names or commercial products constitute an endorsement or recommendation of their use.

Acknowledgements. We thank the Hong Kong Environmental Protection Department for providing us with the data. This work was supported by the Natural Science Foundation of China (41275122), the Research Grants Council (RGC) of the Hong Kong Government of Special Administrative Region (PolyU5154/13E, PolyU152052/14E, PolyU152052/16E and CRF/C5004-15E), the Innovation and Technology Commission of the HKSAR to the Hong Kong Branch of National Rail Transit Electrification and Automation Engineering Technology Research Center, and the Hong Kong Polytechnic University PhD scholarships (project #RTTA). This study is partly supported by the Hong Kong PolyU internal grant (1-BBW4 and 1-BBYD).

Edited by: Andreas Hofzumahaus
Reviewed by: two anonymous referees

References

Atkinson, R. and Arey, J.: Atmospheric degradation of volatile organic compounds, Chem. Rev., 103, 4605–4638, 2003.

Barletta, B., Meinardi, S., Simpson, I. J., Khwaja, H. A., Blake, D. R., and Rowland, F. S.: Mixing ratios of volatile organic compounds (VOCs) in the atmosphere of Karachi, Pakistan, Atmos. Environ., 36, 3429–3443, 2002.

Beirle, S., Boersma, K. F., Platt, U., Lawrence, M. G., and Wagner, T.: Megacity Emissions and Lifetimes of Nitrogen Oxides Probed from Space, Science, 333, 1737–1739, 2011.

Borbon, A., Fontaine, H., Veillerot, M., Locoge, N., Galloo, J. C., and Guillermo, R.: An investigation into the traffic-related fraction of isoprene at an urban location, Atmos. Environ., 35, 3749–3760, 2001.

Cardelino, C. A. and Chameides, W. L.: An Observation-Based Model for Analyzing Ozone Precursor Relationships in the Urban Atmosphere, J. Air Waste Manage., 45, 161–180, https://doi.org/10.1080/10473289.1995.10467356, 1995.

Carslaw, D. C.: Evidence of an increasing NO_2 / NO_x emissions ratio from road traffic emissions, Atmos. Environ., 39, 4793–4802, 2005.

Chan, L. Y., Chan, C. Y., and Qin, Y.: Surface ozone pattern in Hong Kong, J. Appl. Meteorol., 37, 1153–1165, 1998a.

Chan, L. Y., Liu, H. Y., Lam, K. S., Wang, T., Oltmans, S. J., and Harris, J. M.: Analysis of the seasonal behavior of tropospheric ozone at Hong Kong, Atmos. Environ., 32, 159–168, 1998b.

Cheng, H. R., Guo, H., Wang, X. M., Saunders, S. M., Lam, S. H., Jiang, F., Wang, T. J., Ding, A. J., Lee, S. C., and Ho, K. F.: On the relationship between ozone and its precursors in the Pearl River Delta: application of an observation-based model (OBM), Environ. Sci. Pollut. R., 17, 547–560, 2010.

Cheng, H. R., Saunders, S. M., Guo, H., Louie, P. K., and Jiang, F.: Photochemical trajectory modeling of ozone concentrations in Hong Kong, Environ. Pollut., 180, 101–110, 2013.

Cheung, K., Guo, H., Ou, J. M., Simpson, I. J., Barletta, B., Meinardi, S., and Blake, D. R.: Diurnal profiles of isoprene, methacrolein and methyl vinyl ketone at an urban site in Hong Kong, Atmos. Environ., 84, 323–331, 2014.

Chou, C. C. K., Liu, S. C., Lin, C. Y., Shiu, C. J., and Chang, K. H.: The trend of surface ozone in Taipei, Taiwan, and its causes: Implications for ozone control strategies, Atmos. Environ., 40, 3898–3908, 2006.

Coates, J. and Butler, T. M.: A comparison of chemical mechanisms using tagged ozone production potential (TOPP) analysis, Atmos. Chem. Phys., 15, 8795–8808, https://doi.org/10.5194/acp-15-8795-2015, 2015.

Cui, J., Pandey Deolal, S., Sprenger, M., Henne, S., Staehelin, J., Steinbacher, M., and Nédélec, P.: Free tropospheric ozone changes over Europe as observed at Jungfraujoch (1990–2008): An analysis based on backward trajectories, J. Geophys. Res., 116, D10304, https://doi.org/10.1029/2010JD015154, 2011.

Dallmann, T. R., Harley, R. A., and Kirchstetter, T. W.: Effects of Diesel Particle Filter Retrofits and Accelerated Fleet Turnover on Drayage Truck Emissions at the Port of Oakland, Environ. Sci. Technol., 45, 10773–10779, 2011.

Derwent, R. G., Manning, A. J., Simmonds, P. G., Spain, T. G., and O'Doherty, S.: Analysis and interpretation of 25 years of ozone observations at the Mace Head Atmospheric Research Station on

the Atlantic Ocean coast of Ireland from 1987 to 2012, Atmos. Environ., 80, 361–368, 2013.

Dils, B.: Long Range Transport of Tropospheric NO_2 as simulated by FLEXPART, Product Specification document TEM/LRT2/001, TEMIS, De Bilt, The Netherlands, 2008.

Ding, A. J., Wang, T., Zhao, M., Wang, T. J., and Li, Z. K.: Simulation of sea-land breezes and a discussion of their implications on the transport of air pollution during a multi-day ozone episode in the Pearl River Delta of China, Atmos. Environ., 38, 6737–6750, 2004.

Ding, A. J., Wang, T., Thouret, V., Cammas, J.-P., and Nédélec, P.: Tropospheric ozone climatology over Beijing: analysis of aircraft data from the MOZAIC program, Atmos. Chem. Phys., 8, 1–13, https://doi.org/10.5194/acp-8-1-2008, 2008.

Evans, M. J. and Jacob, D. J.: Impact of new laboratory studies of N2O5 hydrolysis on global model budgets of tropospheric nitrogen oxides, ozone, and OH, Geophys. Res. Lett., 32, L09813, https://doi.org/10.1029/2005GL022469, 2005.

GDEMC and HKEPD (Guangdong Environmental Monitoring Centre and Hong Kong Environmental Protection Department): Pearl River Delta Regional Air Quality Monitoring Network – A Report of Monitoring Results in 2014, available at: http://www.epd.gov.hk/epd/english/resources_pub/publications/m_report.html (last access: 10 September 2017), 2015.

Geddes, J. A., Murphy, J. G., and Wang, D. K.: Long term changes in nitrogen oxides and volatile organic compounds in Toronto and the challenges facing local ozone control, Atmos. Environ., 43, 3407–3415, 2009.

George, I. J., Matthews, P. S. J., Whalley, L. K., Brooks, B., Goddard, A., Baeza-Romero, M. T., and Heard, D. E.: Measurements of uptake coefficients for heterogeneous loss of HO_2 onto submicron inorganic salt aerosols, Phys. Chem. Chem. Phys., 15, 12829–12845, 2013.

Guo, H., Lee, S. C., Louie, P. K., and Ho, K. F.: Characterization of hydrocarbons, halocarbons and carbonyls in the atmosphere of Hong Kong, Chemosphere, 57, 1363–1372, 2004.

Guo, H., Jiang, F., Cheng, H. R., Simpson, I. J., Wang, X. M., Ding, A. J., Wang, T. J., Saunders, S. M., Wang, T., Lam, S. H. M., Blake, D. R., Zhang, Y. L., and Xie, M.: Concurrent observations of air pollutants at two sites in the Pearl River Delta and the implication of regional transport, Atmos. Chem. Phys., 9, 7343–7360, https://doi.org/10.5194/acp-9-7343-2009, 2009.

Guo, H., Ling, Z. H., Cheung, K., Jiang, F., Wang, D. W., Simpson, I. J., Barletta, B., Meinardi, S., Wang, T. J., Wang, X. M., Saunders, S. M., and Blake, D. R.: Characterization of photochemical pollution at different elevations in mountainous areas in Hong Kong, Atmos. Chem. Phys., 13, 3881–3898, https://doi.org/10.5194/acp-13-3881-2013, 2013.

HKEPD (Hong Kong Environmental Protection Department): Air Quality in Hong Kong 2014, available at: http://www.aqhi.gov.hk/api_history/english/report/files/AQR2014e_Update0616.pdf (last access: 10 September 2017), 2015.

HKEPD (Hong Kong Environmental Protection Department): 2014 Hong Kong Emission Inventory Report, available at: http://www.epd.gov.hk/epd/sites/default/files/epd/2014Summary_of_Updates_eng_2.pdf (last access: 10 September 2017), 2016.

Ho, K. F., Lee, S. C., Ho, W. K., Blake, D. R., Cheng, Y., Li, Y. S., Ho, S. S. H., Fung, K., Louie, P. K. K., and Park, D.: Vehicular emission of volatile organic compounds (VOCs) from a tunnel study in Hong Kong, Atmos. Chem. Phys., 9, 7491–7504, https://doi.org/10.5194/acp-9-7491-2009, 2009.

Huang, J. P., Fung, J. C. H., Lau, A. K. H., and Qin, Y.: Numerical simulation and process analysis of typhoon-related ozone episodes in Hong Kong, J. Geophys. Res., 110, D05301, https://doi.org/10.1029/2004JD004914, 2005.

Itano, Y., Bandow, H., Takenaka, N., Saitoh, Y., Asayama, A., and Fukuyama, J.: Impact of NOx reduction on long-term ozone trends in an urban atmosphere, Sci. Total Environ., 379, 46–55, 2007.

Jenkin, M. E., Saunders, S. M., and Pilling, M. J.: The tropospheric degradation of volatile organic compounds: a protocol for mechanism development, Atmos. Environ., 31, 81–104, 1997.

Jenkin, M. E., Saunders, S. M., Wagner, V., and Pilling, M. J.: Protocol for the development of the Master Chemical Mechanism, MCM v3 (Part B): tropospheric degradation of aromatic volatile organic compounds, Atmos. Chem. Phys., 3, 181–193, https://doi.org/10.5194/acp-3-181-2003, 2003.

Jiang, F., Guo, H., Wang, T. J., Cheng, H. R., Wang, X. M., Simpson, I. J., Ding, A. J., Saunders, S. M., Lam, S. H. M., and Blake, D. R.: An ozone episode in the Pearl River Delta: Field observation and model simulation, J. Geophys. Res., 115, D22305, https://doi.org/10.1029/2009JD013583, 2010.

Lakey, P. S. J., George, I. J., Whalley, L. K., Baeza-Romero, M. T., and Heard, D. E.: Measurements of the HO_2 Uptake Coefficients onto Single Component Organic Aerosols, Environ. Sci. Technol., 49, 4878–4885, 2015.

Lam, S. H. M., Saunders, S. M., Guo, H., Ling, Z. H., Jiang, F., Wang, X. M., and Wang, T. J.: Modelling VOC source impacts on high ozone episode days observed at a mountain summit in Hong Kong under the influence of mountain-valley breezes, Atmos. Environ., 81, 166–176, 2013.

Lau, C. F., Rakowska, A., Townsend, T., Brimblecombe, P., Chan, T. L., Yam, Y. S., Mocnik, G., and Ning, Z.: Evaluation of diesel fleet emissions and control policies from plume chasing measurements of on-road vehicles, Atmos. Environ., 122, 171–182, 2015.

Lee, Y. C., Shindell, D. T., Faluvegi, G., Wenig, M., Lam, Y. F., Ning, Z., Hao, S., and Lai, C. S.: Increase of ozone concentrations, its temperature sensitivity and the precursor factor in South China, Tellus B, 66, 23455, https://doi.org/10.3402/tellusb.v66.23455, 2014.

Lefohn, A. S., Shadwick, D., and Oltmans, S. J.: Characterizing changes in surface ozone levels in metropolitan and rural areas in the United States for 1980–2008 and 1994–2008, Atmos. Environ., 44, 5199–5210, 2010.

Li, J. F., Lu, K. D., Lv, W., Li, J., Zhong, L. J., Ou, Y. B., Chen, D. H., Huang, X., and Zhang, Y. H.: Fast increasing of surface ozone concentrations in Pearl River Delta characterized by a regional air quality monitoring network during 2006–2011, J. Environ. Sci., 26, 23–36, 2014.

Lin, M., Horowitz, L. W., Payton, R., Fiore, A. M., and Tonnesen, G.: US surface ozone trends and extremes from 1980 to 2014: quantifying the roles of rising Asian emissions, domestic controls, wildfires, and climate, Atmos. Chem. Phys., 17, 2943–2970, https://doi.org/10.5194/acp-17-2943-2017, 2017.

Ling, Z. H., Guo, H., Cheng, H. R., and Yu, Y. F.: Sources of ambient volatile organic compounds and their contributions to photochemical ozone formation at a site in the Pearl River Delta, southern China, Environ. Pollut., 159, 2310–2319, 2011.

Ling, Z. H., Guo, H., Zheng, J. Y., Louie, P. K. K., Cheng, H. R., Jiang, F., Cheung, K., Wong, L. C., and Feng, X. Q.: Establishing a conceptual model for photochemical ozone pollution in subtropical Hong Kong, Atmos. Environ., 76, 208–220, 2013.

Ling, Z. H., Guo, H., Lam, S. H. M., Saunders, S. M., and Wang, T.: Atmospheric photochemical reactivity and ozone production at two sites in Hong Kong: Application of a Master Chemical Mechanism-photochemical box model, J. Geophys. Res., 119, 10567–10582, 2014.

Louie, P. K. K., Zhong, L. J., Zheng, J. Y. A., and Lau, A. K. H.: A Special Issue of Atmospheric Environment on "Improving Regional Air Quality over the Pearl River Delta and Hong Kong: From Science to Policy", Atmos. Environ., 76, 1–2, 2013.

Lu, K. D., Zhang, Y. H., Su, H., Brauers, T., Chou, C. C., Hofzumahaus, A., Liu, S. C., Kita, K., Kondo, Y., Shao, M., Wahner, A., Wang, J. L., Wang, X. S., and Zhu, T.: Oxidant (O_3+NO_2) production processes and formation regimes in Beijing, J. Geophys. Res., 115, D07303, https://doi.org/10.1029/2009JD012714, 2010.

Lyu, X., Guo, H., Simpson, I. J., Meinardi, S., Louie, P. K. K., Ling, Z., Wang, Y., Liu, M., Luk, C. W. Y., Wang, N., and Blake, D. R.: Effectiveness of replacing catalytic converters in LPG-fueled vehicles in Hong Kong, Atmos. Chem. Phys., 16, 6609–6626, https://doi.org/10.5194/acp-16-6609-2016, 2016.

Lyu, X. P., Chen, N., Guo, H., Zhang, W. H., Wang, N., Wang, Y., and Liu, M.: Ambient volatile organic compounds and their effect on ozone production in Wuhan, central China, Sci. Total Environ., 541, 200–209, 2015a.

Lyu, X. P., Ling, Z. H., Guo, H., Saunders, S. M., Lam, S. H. M., Wang, N., Wang, Y., Liu, M., and Wang, T.: Re-examination of C1–C5 alkyl nitrates in Hong Kong using an observation-based model, Atmos. Environ., 120, 28–37, 2015b.

Lyu, X. P., Zeng, L. W., Guo, H., Simpson, I. J., Ling, Z. H., Wang, Y., Murray, F., Louie, P. K. K., Saunders, S. M., Lam, S. H. M., and Blake, D. R.: Evaluation of the effectiveness of air pollution control measures in Hong Kong, Environ. Pollut., 220, 87–94, 2017.

Madronich, S. and Flocke, S.: The Role of Solar Radiation in Atmospheric Chemistry, Handbook of Environmental Chemistry, Vol. 2 Part L, Springer-Verlag, Berlin, German, 1999.

Merlaud, A., Van Roozendael, M., Theys, N., Fayt, C., Hermans, C., Quennehen, B., Schwarzenboeck, A., Ancellet, G., Pommier, M., Pelon, J., Burkhart, J., Stohl, A., and De Mazière, M.: Airborne DOAS measurements in Arctic: vertical distributions of aerosol extinction coefficient and NO2 concentration, Atmos. Chem. Phys., 11, 9219–9236, https://doi.org/10.5194/acp-11-9219-2011, 2011.

Ning, Z., Wubulihairen, M., and Yang, F.: PM, NO_x and butane emissions from on-road vehicle fleets in Hong Kong and their implications on emission control policy, Atmos. Environ., 61, 265–274, 2012.

Oltmans, S. J., Lefohn, A. S., Shadwick, D., Harris, J. M., Scheel, H. E., Galbally, I., Tarasick, D. W., Johnson, B. J., Brunke, E. G., Claude, H., Zeng, G., Nichol, S., Schmidlin, F., Davies, J., Cuevas, E., Redondas, A., Naoe, H., Nakano, T., and Kawasato, T.: Recent tropospheric ozone changes – A pattern dominated by slow or no growth, Atmos. Environ., 67, 331–351, 2013.

Ou, J. M., Guo, H., Zheng, J. Y., Cheung, K., Louie, P. K. K., Ling, Z. H., and Wang, D. W.: Concentrations and sources of non-methane hydrocarbons (NMHCs) from 2005 to 2013 in Hong Kong: A multi-year real-time data analysis, Atmos. Environ., 103, 196–206, 2015.

Parrish, D. D., Law, K. S., Staehelin, J., Derwent, R., Cooper, O. R., Tanimoto, H., Volz-Thomas, A., Gilge, S., Scheel, H.-E., Steinbacher, M., and Chan, E.: Long-term changes in lower tropospheric baseline ozone concentrations at northern mid-latitudes, Atmos. Chem. Phys., 12, 11485–11504, https://doi.org/10.5194/acp-12-11485-2012, 2012.

Pollack, I. B., Ryerson, T. B., Trainer, M., Neuman, J. A., Roberts, J. M., and Parrish, D. D.: Trends in ozone, its precursors, and related secondary oxidation products in Los Angeles, California: A synthesis of measurements from 1960 to 2010, J. Geophys. Res., 118, 5893–5911, 2013.

Reimann, S., Calanca, P., and Hofer, P.: The anthropogenic contribution to isoprene concentrations in a rural atmosphere, Atmos. Environ., 34, 109–115, 2000.

Rivera, C., Stremme, W., and Grutter, M.: Nitrogen dioxide DOAS measurements from ground and space: comparison of zenith scattered sunlight ground-based measurements and OMI data in Central Mexico, Atmósfera, 26, 401–414, 2013.

Saunders, S. M., Jenkin, M. E., Derwent, R. G., and Pilling, M. J.: Protocol for the development of the Master Chemical Mechanism, MCM v3 (Part A): tropospheric degradation of non-aromatic volatile organic compounds, Atmos. Chem. Phys., 3, 161–180, https://doi.org/10.5194/acp-3-161-2003, 2003.

Seinfeld, J. H. and Pandis, S. N.: Atmos. Chem. Phys.: from air pollution to climate change, 2nd Edn., Wiley Publisher, New Jersey, USA, 2006.

Sillman, S.: The relation between ozone, NO_x and hydrocarbons in urban and polluted rural environments, Atmos. Environ., 33, 1821–1845, 1999.

Simpson, I. J., Blake, N. J., Barletta, B., Diskin, G. S., Fuelberg, H. E., Gorham, K., Huey, L. G., Meinardi, S., Rowland, F. S., Vay, S. A., Weinheimer, A. J., Yang, M., and Blake, D. R.: Characterization of trace gases measured over Alberta oil sands mining operations: 76 speciated C_2–C_{10} volatile organic compounds (VOCs), CO_2, CH_4, CO, NO, NO_2, NO_y, O_3 and SO_2, Atmos. Chem. Phys., 10, 11931–11954, https://doi.org/10.5194/acp-10-11931-2010, , 2010.

So, K. L. and Wang, T.: On the local and regional influence on ground-level ozone concentrations in Hong Kong, Environ. Pollut., 123, 307–317, 2003.

So, K. L. and Wang, T.: C3-C12 non-methane hydrocarbons in subtropical Hong Kong: spatial-temporal variations, source-receptor relationships and photochemical reactivity, Sci. Total Environ., 328, 161–174, 2004.

Tang, G., Li, X., Wang, Y., Xin, J., and Ren, X.: Surface ozone trend details and interpretations in Beijing, 2001–2006, Atmos. Chem. Phys., 9, 8813–8823, https://doi.org/10.5194/acp-9-8813-2009, 2009.

Tanimoto, H.: Increase in springtime tropospheric ozone at a mountainous site in Japan for the period 1998–2006, Atmos. Environ., 43, 1358–1363, 2009.

TF HTAP (Task Force on Hemispheric Transport of Air Pollution): Hemispheric Transport of Air Pollution 2010, Part A. Ozone and Particulate Matter, United Nations Economic Commission for Europe, Geneva, 304 pp., 2010.

Tian, L. W., Hossain, S. R., Lin, H. L., Ho, K. F., Lee, S. C., and Yu, I. T. S.: Increasing trend of primary NO2 exhaust emission fraction in Hong Kong, Environ. Geochem. Hlth., 33, 623–630, 2011.

Tsai, W. Y., Chan, L. Y., Blake, D. R., and Chu, K. W.: Vehicular fuel composition and atmospheric emissions in South China: Hong Kong, Macau, Guangzhou, and Zhuhai, Atmos. Chem. Phys., 6, 3281–3288, https://doi.org/10.5194/acp-6-3281-2006, 2006.

Tsui, J. K.-Y., Guenther, A., Yip, W.-K., and Chen, F.: A biogenic volatile organic compound emission inventory for Hong Kong, Atmos. Environ., 43, 6442–6448, 2009.

Wang, N., Guo, H., Jiang, F., Ling, Z. H., and Wang, T.: Simulation of ozone formation at different elevations in mountainous area of Hong Kong using WRF-CMAQ model, Sci. Total Environ., 505, 939–951, 2015.

Wang, T. and Kwok, J. Y. H.: Measurement and analysis of a multiday photochemical smog episode in the Pearl River delta of China, J. Appl. Meteorol., 42, 404–416, 2003.

Wang, T., Guo, H., Blake, D. R., Kwok, Y. H., Simpson, I. J., and Li, Y. S.: Measurements of Trace Gases in the Inflow of South China Sea Background Air and Outflow of Regional Pollution at Tai O, Southern China, J. Atmos. Chem., 52, 295–317, 2005.

Wang, T., Wei, X. L., Ding, A. J., Poon, C. N., Lam, K. S., Li, Y. S., Chan, L. Y., and Anson, M.: Increasing surface ozone concentrations in the background atmosphere of Southern China, 1994–2007, Atmos. Chem. Phys., 9, 6217–6227, https://doi.org/10.5194/acp-9-6217-2009, 2009.

Wang, X. M., Liu, H., Pang, J. M., Carmichael, G., He, K. B., Fan, Q., Zhong, L. J., Wu, Z. Y., and Zhang, J. P.: Reductions in sulfur pollution in the Pearl River Delta region, China: Assessing the effectiveness of emission controls, Atmos. Environ., 76, 113–124, 2013.

Xu, X., Lin, W., Wang, T., Yan, P., Tang, J., Meng, Z., and Wang, Y.: Long-term trend of surface ozone at a regional background station in eastern China 1991–2006: enhanced variability, Atmos. Chem. Phys., 8, 2595–2607, https://doi.org/10.5194/acp-8-2595-2008, 2008.

Xue, L. K., Wang, T., Louie, P. K., Luk, C. W., Blake, D. R., and Xu, Z.: Increasing external effects negate local efforts to control ozone air pollution: a case study of Hong Kong and implications for other chinese cities, Environ. Sci. Technol., 48, 10769–10775, 2014.

Yao, X., Lau, N. T., Chan, C. K., and Fang, M.: The use of tunnel concentration profile data to determine the ratio of NO_2 / NO_x directly emitted from vehicles, Atmos. Chem. Phys. Discuss., https://doi.org/10.5194/acpd-5-12723-2005, 2005.

Yarwood, G., Rao, S.,Yocke, M., and Whitten, G. Z.: Updates to the Carbon Bond Chemical Mechanism: CB05, Tech. rep., US Environmental Protection Agency, Novato, California, USA, 2005.

Zhang, J., Wang, T., Chameides, W. L., Cardelino, C., Kwok, J., Blake, D. R., Ding, A., and So, K. L.: Ozone production and hydrocarbon reactivity in Hong Kong, Southern China, Atmos. Chem. Phys., 7, 557–573, https://doi.org/10.5194/acp-7-557-2007, 2007.

Zhang, Q., Yuan, B., Shao, M., Wang, X., Lu, S., Lu, K., Wang, M., Chen, L., Chang, C.-C., and Liu, S. C.: Variations of ground-level O_3 and its precursors in Beijing in summertime between 2005 and 2011, Atmos. Chem. Phys., 14, 6089–6101, https://doi.org/10.5194/acp-14-6089-2014, 2014.

Zhong, L. J., Louie, P. K. K., Zheng, J. Y., Yuan, Z. B., Yue, D. L., Ho, J. W. K., and Lau, A. K. H.: Science-policy interplay: Air quality management in the Pearl River Delta region and Hong Kong, Atmos. Environ., 76, 3–10, 2013.